ROYAL SOCIETY OF CHEMISTRY

PAPER

Check for updates

Ion conduction and phase behaviour in dual cation polyelectrolyte blends for sodium-ion batteries†

Sneha Malunavar,[a] Luca Porcarelli,*[a,b] Patrick C. Howlett,[a] David Mecerreyes[b,c] and Maria Forsyth*[a,b,c]

Emerging battery technologies such as solid-state sodium batteries can benefit from new polymer electrolytes with improved sodium ion transport to optimise electrochemical performance. In this work, we propose, for the first time, the use of polyelectrolyte blends utilising a dual cation approach with a common polyanion backbone, poly(1-[3-(methacryloyloxy)propylsulfonyl]-1-(trifluoromethanesulfonyl) imide) (polyMTFSI). Thus, three new anionic polyelectrolytes were synthesised based on polyMTFSI having three different counter cations such as sodium (Na) (polyMTFSI-Na), trimethyl(isobutyl)phosphonium (poly-MTFSIP$_{111i4}$) and diethyl (isobutyl)(methyl)phosphonium (polyMTFSI-P$_{122i4}$). The miscibility between the polyelectrolytes in blends was determined by observing a single glass transition, T_g, for different compositions. Upon the addition of bulky organic cations, an increase in the dynamics and ionic conductivity was observed. Finally, we investigated the effect of NaFSI as an additional component in a ternary electrolyte system, whereby the salt acted as a plasticizer, decreasing T_g, and further enhancing the ionic conductivity.

Introduction

Research into new energy storage systems is gaining increasing importance compared with any time in the past. In particular, efforts to improve the lithium (Li)/sodium (Na) ion battery technology are seen as paramount due to their high specific energy and energy density (per unit volume)[1,2] compared to other technologies. With the electrolyte being the key component of any electrochemical device, research has been focusing on the development of new electrolytes with improved performance in addition to being cost effective and safe in batteries. One effective way to improve the safety of batteries is by developing solid polymer electrolytes (SPEs) having both good ion transport and robust mechanical properties.[3–5] Solid-state electrolytes are promising compared to liquid electrolytes in terms of non-flammability, no leakage issues, and good mechanical properties, and they serve as both the electrolyte and the separator. The different classes of solid-state electrolytes are solid polymer electrolytes, gel polymer electrolytes, inorganic electrolytes, and composites. Despite their advantages,

they are still in the early stages of research and development compared to liquid electrolytes, and the current solid-state Na electrolytes have low ionic conductivity at room temperature, and there have been some attempts to increase their ionic conductivity by incorporating various additives. There is a lot of research around the development of solid-state electrolytes for lithium-ion batteries but not as much progress has been made for SIB applications. Therefore, developing a solid-state electrolyte for SIB applications is the main goal of this work.[8–10]

In the 1970s, Wright *et al.*[6] reported SPEs comprised of PEO and alkali salts such as NaI. Later, Armand *et al.*[7] reported SPEs for Li-ion conducting systems with weakly coordinating anions (bis(trifluoromethanesulfonyl)imide, TFSI⁻) forming a flexible molecular structure, hypothesising that the selection of such anions for making Li conducting SPEs would be beneficial for practical lithium metal batteries (LMBs).

Traditional SPEs usually consist of Li/Na salts dissolved in a polymer host; these are commonly recognised as dual-ion conductors, in which case both alkali metal cations and the accompanying anions will be mobile. In most cases anions are more mobile than the metal cations, which accounts for the low transference number in dual ion conducting SPEs, usually being much lower than 0.5, as has been demonstrated in extensive studies on these SPEs.[8,10–15] This kind of dual ion conducting SPE tends to have drawbacks during the cycling of the cell, as both the ions are moving and the anions tend to accumulate at the positive electrode causing a concentration gradient which leads to cell polarization and results in poor

[a]Institute for Frontier Materials (IFM) Deakin University, Burwood, Victoria 3125, Australia. E-mail: maria.forsyth@deakin.edu.au
[b]Polymat, University of the Basque Country UPV/EHU, Joxe Mari Korta Center, Avda, Tolosa 7, 20018 Donostia-San Sebastian, Spain
[c]Ikerbasque, Basque Foundation for Science, 48013 Bilbao, Spain

cell performance, voltage loses, high internal impedance along with unexpected reactions during cycling and finally leading to cell death.[16] One way to overcome these issues would be to develop SPEs which possess a metal ion transference number equal to unity, so-called single ion conductors. Fuller et al.[17] demonstrated that polymer electrolytes with a transference number equal to 1 showed overall good performance even with a conductivity decrease by one order. Therefore, there is interest in developing single ion conducting SPEs to overcome the above-mentioned challenges caused by the dual ion conducing SPEs, at the very least to reduce or eliminate anion conductivity in SPEs.

Bannister et al.,[18] in the 1980s, came up with two ways to design single Li-ion conducting SPEs. One way is to tether the anion to the polymer backbone; in this way the anion will be covalently bound to the polymer backbone, eliminating its contribution to conductivity (and hence its transference number is zero) and allowing the counter cation to be the sole charge carrier in the electrolyte. Another way is to use Li salts where the mobility of the anion is inhibited. Since then, there have been various reports on such SPEs with Armand et al.[19] having extensively reviewed the various synthetic strategies and designs of single ion conducting SPEs with a high transference number and high ionic conductivities for lithium-ion batteries. Zheng et al.[20] reported sodium ion single ion conducting SPEs consisting of poly(sodium 2-[μ-metharyloyloligo(oxyethylene)] ethylsulfonate); in this system, the oligo(oxyethylene) chain assists in the dissociation of the sodium cation from sulfonate and Na$^+$ ion transport is facilitated by flexible macromolecular chains.

In all cases, the ion motion in these SPEs is governed by the local segmental motion of the polymer as reflected in the glass transition (T_g). However, it is difficult to achieve both high ionic conductivity and good mechanical properties if the design requires T_g to be low. Another approach is to design SPEs where ions are mobile below the T_g and hence decoupling ionic conductivity from polymer segmental motion. Using this strategy, Mohd Noor et al.[21] reported SPEs composed of poly-([triethylmethylammonium][2-acrylamido-2-methyl-1-propanesulfonicacid]-co-sodium[vinyl sulfonate]), poly([N1222][AMPS]-co-Na[VS]); here some fractions of sodium ions were replaced by a bulky quaternary ammonium cation. The intention here was to decrease the strong interactions between the Na cations and the anions on the polymer backbone by replacing some of the interacting cations with bulky organic cations. They found this approach to be partially successful with considerable ionic conductivity measured below the glass transition temperature of the polymers; this indicated that the ion transport mechanism was indeed decoupled from the structural relaxations of the polymer. The hypothesis was that the addition of the bulky cation increased the free volume in the polymer matrix and created a 'looser' ionic structure facilitating sodium ion hopping. They further extended their study to another system, poly(2-acryl-amido-2-methyl-1-propane-sulfonate) homopolymer (PAMPS), where they also reported significant conductivity below the T_g, with

the highest conductivity being achieved by 10 : 90 mol% of Na$^+$/triethylmethylammonium (N$_{1222}$) cations.[22] They observed similar trends of decoupling in all these co-cation systems and found that conductivity is improved when the organic cation is bulkier. Unfortunately, the ionic conductivities reported were much lower than required for practical device applications due to the strong bonding between the sulfonate anions on the backbone and the metal cations. Interestingly, when a small amount of tetraglyme (~10 wt%) was incorporated as a plasticizer, this resulted in a jump in ionic conductivity by several orders while still retaining a high T_g. There are additional reports in the literature based on this hypothesis; however, all rely on the sulfonate anion on the polyelectrolyte,[23,24] and designing systems with a more delocalised anion to decrease the interionic binding energy is hypothesised as a possible way forward with this concept to develop Na$^+$ conducting electrolytes for Na battery applications.

Therefore, in the present work, we investigated mixed co-cation SPEs where the 1-[3-(methacryloyloxy)propylsulfonyl]-1-(trifluoromethanesulfonyl)imide anion is tethered to the polymer backbone. The structure of this moiety is related to the bis(trifluoromethanesulfonyl) or TFSI anion that is known to have a more delocalised charge and leads to improved conductivity in dual ion conductors. Furthermore, instead of copolymerizing different monomers, we investigated the use of blends between different polyelectrolytes having different counter cations. For this purpose, three methacrylic sulfonamide polyelectrolytes with different counter cations, namely sodium and two bulky phosphonium cations, were synthesized as shown in Scheme 1. The blends between the different polyelectrolytes were investigated with a focus on their miscibility, glass transition temperature, ionic conductivity, mechanical behaviour, and their inter-relationships. We also investigated the effect of adding NaFSI to the most conductive polyelectrolyte blend composition to further enhance the ionic conductivity and present preliminary electrochemical properties for this material.

Results and discussion

The synthetic route for the preparation of the monomers is shown in Scheme 1. The NaMTFSI monomer was synthesised by following 3 steps as reported previously for the LiMTFSI monomer by Porcarelli et al. and Shaplov et al.[25,26] Then, the corresponding three homopolymers were synthesized by free-radical polymerization. The chemical structure is shown in Scheme 1, with a common polyanion backbone, poly(1-[3-(methacryloyloxy)propylsulfonyl]-1-(trifluoromethanesulfonyl)imide) (polyMTFSI), having three different counter cations such as sodium (Na) (polyMTFSI-Na), trimethyl(isobutyl)phosphonium (poly-MTFSIP$_{111i4}$) and diethyl (isobutyl)(methyl) phosphonium (polyMTFSI-P$_{122i4}$).

In this work, a series of blends between two different polyelectrolytes having the same polymer backbone but different counterions were systematically prepared and characterised.

© 2024 The Author(s). Published by the Royal Society of Chemistry

RSC Appl. Polym., 2024, 2, 384–394 | 385

Scheme 1 Structure of polymers NaMTFSI **7**, P_{111i4}MTFSI **8** and P_{122i4}MTFSI **9**.

**Table 1** Polymer blends of poly-NaMTFSI with either poly-P_{111i4}MTFSI or poly-P_{122i4}MTFSI (mol%)

Poly-NaMTFSI (mol%)	Poly-P_{111i4}MTFSI (mol%) OR poly-P_{122i4}MTFSI (mol%)
100	0
75	25
50	50
25	75
0	100

Specifically, poly-NaMTFSI **7** was blended by simple co-casting from a common solvent (acetonitrile) with two different phosphonium based polyelectrolytes **8** and **9**. The ratios of the polymer blends that were considered are provided in Table 1.

Characterization of polyelectrolyte blends

The miscibility of the polyelectrolyte blends was investigated by measuring the glass transition temperature using differential scanning calorimetry (DSC). Fig. 1(a) shows the DSC thermograms of the homopolymer poly-NaMTFSI and its polymer blend with 50:50 (mol%) poly-P_{111i4}MTFSI and poly-P_{122i4}MTFSI. The T_g mid-point was determined and plotted in Fig. 1b. It can be observed that neat poly-NaMTFSI has a T_g of around 121 °C, much higher than that of the polymer with counter ion Li$^+$.[26] The polymer blends show only one T_g by DSC, which confirms the miscibility between the individual polymer components in these polymer blends. Compared to the poly-NaMTFSI homopolymers, the blends show a lower T_g in the case of poly-P_{122i4}MTFSI (66 °C) compared to poly-P_{111i4}MTFSI (72 °C). This is the expected behaviour as P_{122i4} is a bulkier group than P_{111i4} and previous studies with ammonium cations in related polyelectrolyte systems have shown a similar trend of decreasing T_g.[22–24] Furthermore, a previous study by Tudryn et al.[28] shows that the T_g decreases in polyester-sulfonate polyelectrolytes with increasing counter cation size; the two factors suggested by Tudryn et al. are the following: (i) bulkier cations act as plasticizers, which help in lowering the T_g of the mixtures and increasing the free volume for ion dynamics, and (ii) bulkier cations are less associated with anions in the backbone, which in turn form weak physical crosslinks that lead to a decrease in the T_g. The T_g broad-
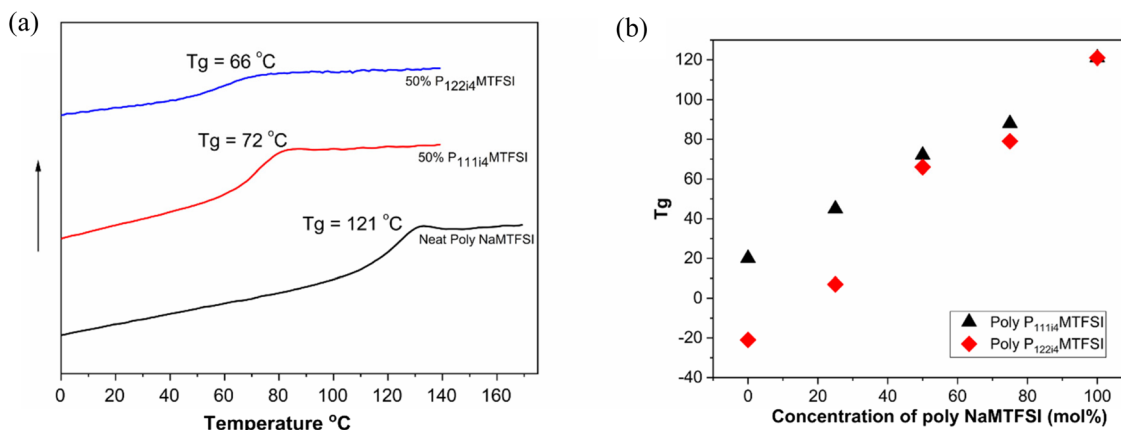
Fig. 1 (a) DSC thermograms of neat poly-NaMTFSI and 50 mol% poly-P_{111i4}MTFSI and poly-P_{122i4}MTFSI polymer blends. (b) T_g of different polymer blends with poly-NaMTFSI with both poly-P_{111i4}MTFSI and P_{122i4}MTFSI at different compositions. Scan rate: 10 K min^{-1}.

ens with the addition of the bulky cation, but P_{122i4} shows more prominent broadening, inferring the possible heterogeneity in this polymer blend, *i.e.* while the system can be considered miscible as per the evidence of a single T_g, the molecular level there will still be heterogeneous. This is also discussed later in the context of the DMA measurement.

Fig. 1(b) shows the composition dependence of the blend T_g for both P_{111i4} and P_{122i4}. With increasing concentrations of these two cations in the blend with poly-NaMTFSI, a decrease in the T_g is clearly observed. The T_g for P_{122i4} over the entire concentration is lower compared to that of P_{111i4}. The onset, mid-point and end-point temperatures of neat poly-NaMTFSI, 50 mol% P_{111i4}MTFSI and 50 mol% P_{122i4}MTFSI polymer blends are also shown in Table 2. These data more clearly indi-

cate likely heterogeneity in the blends with the P_{122i4} counterion where the T_g spans 35 °C from the onset to the endpoint compared to only 17 and 18 °C for the poly-NaMTFSI homopolymer and 50 mol% poly-P_{111i4}MTFSI, respectively. Furthermore, the composition dependence appears to deviate more from the ideal behaviour for this bulkier cation.

Fig. 2 presents the conductivity data as a function of polyelectrolyte blend composition for different concentrations of poly-NaMTFSI with both poly-P_{111i4}MTFSI and poly-P_{122i4}MTFSI as well as a detailed study of the 50 mol% polymer blends. It can be observed that, as the concentration of the bulky phosphonium cation increased, the ionic conductivity also increased in both systems, P_{111i4}MTFSI and P_{122i4}MTFSI, as shown in Fig. 2(a) and (b), respectively. This suggests that the addition of the bulky cation leads to increased free volume and a looser packing of the polymer chains, which facilitates ion motion. Despite the lower T_g for P_{122i4} relative to the P_{111i4} containing blend, the ionic conductivity was higher in the latter polymer blend for all compositions, which was unexpected given that the larger cation would be expected to further enhance the free volume between the chains. Fig. 2(c) compares the conductivity for the two 50 mol% polymer blends, with the respective T_g for each

Table 2 Onset, mid-point and end-point temperatures of neat poly-NaMTFSI, 50 mol% P_{111i4}MTFSI and 50 mol% P_{122i4}MTFSI polymer blends

Polymers	T_g onset/°C	T_u midpoint/°C	T_g endpoint/°C
Neat poly-NaMTFSI	110	121	128
50% P_{111i4}MTFSI	62	72	80
50% P_{122i4}MTFSI	41	66	76

Fig. 2 Ionic conductivity at different concentrations of poly-NaMTFSI with (a) poly-P_{111i4}MTFSI and (b) poly-P_{122i4}MTFSI, (c) ionic conductivity of 50 mol% polymer blends of the mixed co-cation of poly-P_{111i4} and poly-P_{122i4} with poly-NaMTFSI. (d) Ionic conductivity as a function of the bulky cation with inverse temperature normalized by T_g for each polymer blend.

© 2024 The Author(s). Published by the Royal Society of Chemistry

RSC Appl. Polym., 2024, **2**, 384–394 | **387**

system indicated by an arrow, clearly showing that a lower T_g does not necessarily lead to higher ionic conductivity in these cases. Also evident from Fig. 2(c) is the considerable ion conduction at and below T_g for both the polymer blend chemistries at 50 mol%; in the case of the P_{111i4} cation at T_g, the conductivity approaches 10^{-6} S cm^{-1}, which indicates significant decoupling of cation motion from structural dynamics, *i.e.*, even though the overall dynamics in the material was decreasing as the glass transition temperature was approached, some fractions of the cations were still mobile, thus contributing to the measured ionic conductivity. To better display this, the ionic conductivity is plotted against scaled temperature whereby the influence of T_g is removed (*i.e.* T_g/T), as shown in Fig. 2(d). In the polymer blends investigated here, we see that the conductivity is up to 3 orders of magnitude higher (at T_g) than what would be expected if ionic mobility was coupled to polymer dynamics. These findings are comparable to previous reports,[22–24] which show that ionic conductivity increases with the increasing size of the bulky cation in the system and is highly decoupled from the T_g. What we cannot ascertain here is the relative contributions of the Na$^+$ and the phosphonium cations to the conductivity. It is likely that the organic cations are also mobile although one would imagine that the larger size would make them less likely to contribute to conductivity at or near T_g; the mechanism of conduction in a glass would require a hopping or structural rearrangement for ion motion. We can observe that decoupling is an order of magnitude greater for the smaller P_{111i4} cation containing blends, which is consistent with a greater contribution of the smaller organic cation to the measured ionic conductivity. In traditional SPEs both cations and anions move and make it difficult to analyse the mobility of the cation of interest (Li/Na) in the electrolyte system. The Li/Na cations are less mobile than the counter anions, and this can cause concentration polarisation during cell cycling. Furthermore in the traditional SPE, the ionic conductivity is strongly coupled to the polymer segmental dynamics, whereby the ion motion relies on segmental relaxation, which decreases with increasing T_g.[19,30] The work here

is consistent with previous reports that showed that, using mixtures of co-cations, we can decouple ionic conductivity from polymer segmental motions compared to when a single counter ion is present (either only a Na/Li ion or a bulky cation) as studied in previous reports.[28–30] Interestingly, in blends with increasing organic cation composition, the conductivity is significantly lower even though the T_g is also significantly lower, suggesting increased coupling to structural relaxation and indirectly suggesting that the Na$^+$ cation is contributing substantially to the ionic conductivity in the 25 mol% and 50 mol% P_{122i4}/P_{111i4} containing materials.

Dynamic mechanical analysis (DMA) is a technique that is used to measure mechanical properties and structural relaxations in materials. Herein DMA was carried out to understand the thermomechanical properties of 50 mol% polymer blends with the P_{111i4} and P_{122i4} cations. Several notable characteristics of the different materials can be observed in Fig. 3. Firstly, both polymers display a high modulus (of the order of 10^8 Pa) even up to 80 °C where the ionic conductivity is significant (approaching 10^{-5} S cm^{-1}) and the polymer blend containing P_{111i4} has a slightly higher value compared to the P_{122i4} based polymer blend. This shows that significant ionic conductivity is possible in these materials without compromising the mechanical properties,[31] and indeed this high modulus is maintained until 100 °C, within the required temperature range that might be considered for high temperature Na-ion battery operation. The loss modulus and tan δ also show interesting features, both being quite broad and consistent with a broad T_g, and the P_{122i4} based polymer blend shows two features which are indicative of two different relaxation processes. This also suggests that there is some degree of phase separation at the molecular level in this material, which was also hypothesised in previous di-cation polymers reported by Noor *et al.* and could be more prominent for the larger phosphonium with a greater degree of alkyl substitution.

The relaxation temperature (tan δ) observed in Fig. 3(a) and (b) is due to the weak interactions in the ionic polymer chains which cause a loss of mechanical strength;[32] this is associated
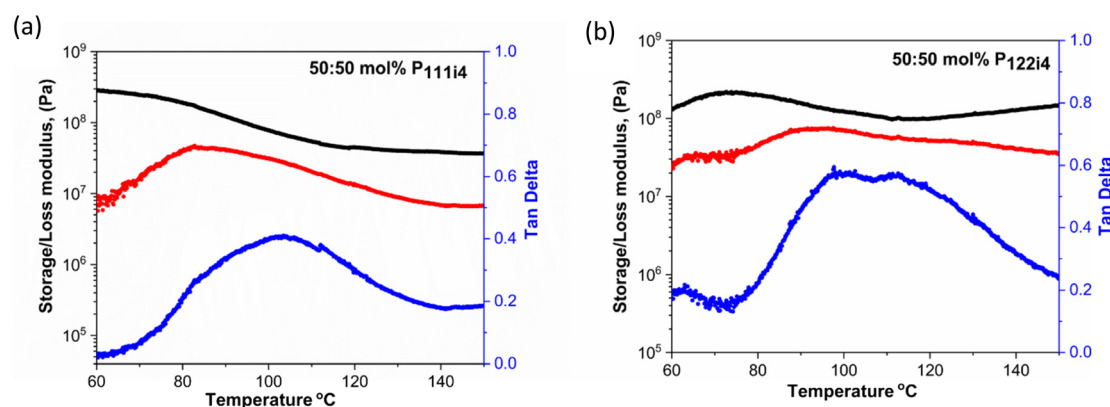

Fig. 3 Storage modulus (*E*′, black), loss modulus (*E*′′, red) and tan δ (blue) as a function of temperature for the 50 mol% polymer blends of the mixed co-cation of poly-NaMTFSI with (a) P_{111i4}MTFSI and (b) P_{122i4}MTFSI.

with the plasticizing effects caused by the addition of bulky cations in the polymer blends.

The data so far suggest that blending anionic polyelectrolytes based on the PMTFSI backbone but with different counterions can be a promising technique to yield significant conductivity below the glass transition temperature of the electrolyte materials and with good mechanical properties, *i.e.*, decoupling ion motion from structural relaxation processes. However, these conductivity values are still not high enough for device applications, so an alternative approach is necessary to boost ion transport.

Previously Mohd Noor *et al.*[33] reported on the effect of the addition of 10% of an organic ether plasticizer to poly ([N_{1222}][AMPS]-*co*-Na[VS]) and poly([N_{1222}][AMPS]-Na)[22] polyelectrolytes. In both cases the ionic conductivity increased significantly, although the effect on T_g was not consistent between the samples, decreasing by 40 °C from the neat copo-

lymer material whereas there was an insignificant change in the ionic conductivity. In another work,[34] the addition of NaFSI salt has been shown to plasticize cationic polyelectrolyte systems based on poly(diallydimethylammonium)bis(trifluoromethanesulfonyl)imide (poly-DADMA) leading to high conductivity values. Such an approach has not been reported previously for the case of anionic polyelectrolytes, which we explore below.

The effect of NaFSI salt in the 50 : 50 mol% polymer blend of poly-P_{111i4}MTFSI and poly-NaMTFSI

The polymer blend of poly-P_{111i4}MTFSI and poly-NaMTFSI was selected to further study the effect of adding NaFSI to the system as this had the highest overall conductivity and decoupled properties as shown above. The main goal was to investigate whether the polyelectrolyte blend could act as a good solvent and further boost ionic conductivity.

The influence of NaFSI salt addition on the T_g of the 50 : 50 mol% polymer blend was studied. All the materials appeared to be brittle solids at room temperature. While the T_g of these systems did decrease even with 10% NaFSI addition (10 wt% NaFSI reduces T_g by 20 °C (56 °C) compared to the neat 50 : 50 polymer blend (72 °C)), the T_g did not vary much with a higher salt concentration, again in contrast to the cationic polyelectrolyte. The determination of T_g is shown in Fig. S2.† Although a broadening of T_g for 20 and 30 mol% salt concentrations is observed, less homogeneity is suggested in these materials, as shown in Fig. 4. This contrasting behaviour between polycationic polyelectrolytes and the present systems suggests a lesser salt solubility in the polyanionic systems and likely different coordination microstructure(s) and phase heterogeneity as areas for possible future investigation in these materials.

Fig. 5(a) shows the ionic conductivity upon the addition of 10, 20 and 30 wt% NaFSI salt to the 50 : 50 polymer blend based on poly-P_{111i4}MTFSI and poly-NaMTFSI. It is clear that
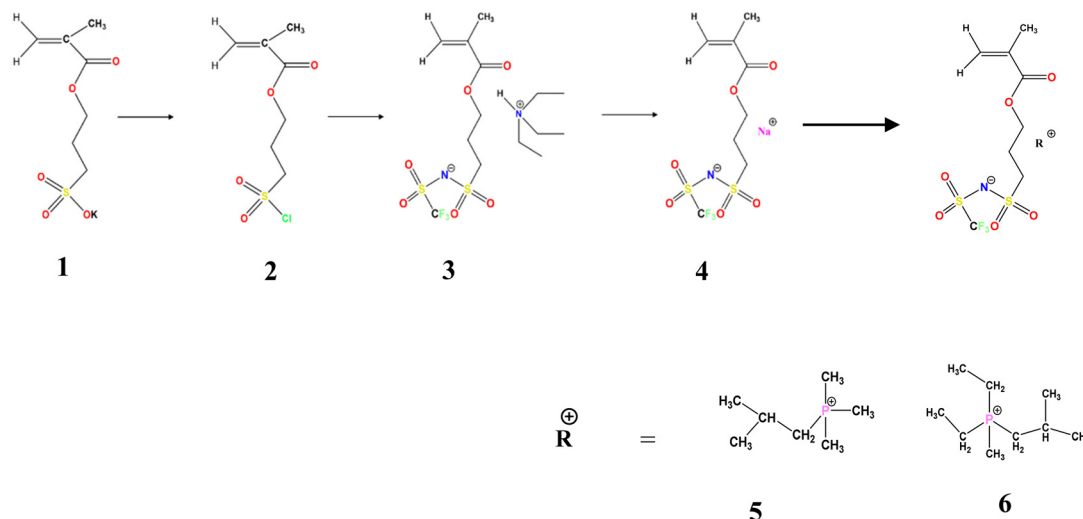

Fig. 4 DSC plot of 50 : 50 mol% polymer blends and the addition of NaFSI salt in wt% at 10 K min^{-1}.

Fig. 5 (a) Ionic conductivity of 50 : 50 mol% polymer blends and the addition of NaFSI salt in wt% at an elevated temperature and (b) ionic conductivity as a function of NaFSI salt concentration with inverse temperature normalized by T_g for each polymer blend.

© 2024 The Author(s). Published by the Royal Society of Chemistry

RSC Appl. Polym., 2024, **2**, 384–394 | **389**

Scheme 2 Synthetic route for the preparation of monomers **4**, **5** and **6**.

the ion conductivity increased over the entire temperature range for all the mixtures with the largest increase in conductivity seen for 30 wt% salt (10^{-6} S cm^{-1}). It is interesting to note that even though the T_g did not vary much from 10 to 30 wt%, the conductivity varied dramatically for each system. When the ionic conductivity was scaled to T_g (Fig. 5(b)), the polymer blend with salts showed recoupling with the polymer backbone, suggesting a change in the conduction mechanism as NaFSI was added. This observation suggests that, whilst the addition of NaFSI salt increased the conductivity, it did not show any improvement in terms of decoupling from the polymer backbone. Thus, further addition of salt was not attempted.

With these peculiar observations, it is difficult to understand which ions are conducting in the system and the relative ion mobility of FSI$^-$, Na$^+$ and the phosphonium cation. Thus, the Na electrochemical behaviour was investigated using the Na/Na symmetric cells discussed below.

The Na/Na symmetric cells were assembled to study the electrochemical properties of the polymer blend in the presence of 30 wt% added NaFSI salt. The sodium transport number, T_{Na^+}, was studied here following the Bruce Vincent method[35] and is shown in Fig. S1.† The result of the electrochemical test showed excellent stability with almost no change in the impedance spectrum before and after polarisation and a value of T_{Na^+} of 0.3 at 70 °C was obtained, indicating that only 30% of the current is attributed to the Na$^+$ ion. This is a little higher than most PEO-based solvent free electrolytes,[36] although still lower compared to other dual cation or single ion conducting polymers. Thus, the addition of NaFSI to this polyanionic electrolyte system leads to a dominant FSI anion conductivity and potentially 'restricts' sodium ion transport, which is again in contrast to previous PDADMAFSI/NaFSI[34] based solid polymer electrolytes and emphasises the importance of molecular composition and architecture in designing next generation solid state polymer electrolyte systems.

Conclusion

We reported herein the use of mixed cation polyelectrolyte blends showing strong decoupling behaviour of conductivity from T_g and mechanical properties. In this work, three methacrylic sulfonamide polyanions with three different counter cations were synthesized, one with a sodium counter cation and two with phosphonium cations of different sizes. The polyelectrolyte blends were miscible in all compositions showing only one glass transition temperature, T_g, and such blending was seen to be a useful method to obtain materials with different counter-cation ratios in a simple way. While the ionic conductivity values for the blends of poly-NaMTFSI with 50 mol% poly-P$_{111i4}$MTFSI and 50 mol% poly-P$_{122i4}$MTFSI were the highest among all the samples prepared, they remained low at approx. 10^{-7} S cm^{-1} at 70 °C. The further addition of NaFSI salt to the polymer blend (poly-NaMTFSI and poly-P$_{111i4}$MTFSI) enhanced the ionic conductivity by up to four orders of magnitude; however, it re-coupled the ion transport to the T_g, suggesting a change in the ion transport mechanism. The T_g was not significantly affected after the first 10 mol% NaFSI addition, which contrasts with the polyelectrolytes with the polycationic backbone and where the anion is the counter-ion. Disappointingly, the sodium cation transference number was low, 0.3 at 70 °C, suggesting that the FSI anion may be the dominant charge carrier. Nevertheless, the work here has shown that blending of polyelectrolytes may be a facile method to create new polymer electrolyte materials with decoupled ion transport, and at the fundamental level, it points to the distinct conduction processes that can eventuate. A deeper understanding of the structure–property relationships in such materials and the transport mechanisms would further advance the field of solid polymer electrolytes for advanced batteries. The in-depth studies to be considered for further understanding of these materials include ion diffusion such as NMR, dielectric spectroscopy and FTIR measurements

390 | *RSC Appl. Polym.*, 2024, **2**, 384–394

© 2024 The Author(s). Published by the Royal Society of Chemistry

and detailed electrochemical analysis of long term charge–discharge cycling.

Experimental

Materials

3-(Chlorosulfonyl)propyl methacrylate (100 g), anhydrous THF ≥ 99.9%, inhibitor free anhydrous DMF 99.8%, dichloromethane, trifluoromethanesulfonamide ($NH_2SO_2CF_3$), triethylamine ≥99.5%, anhydrous magnesium sulfate ≥99.5% (500 g), sodium hydride (NaH), 10 g, dry 90%, 4,4′-azobis(4-cyanovaleric acid) and azobisisobutyronitrile (AIBN) were all purchased from Sigma-Aldrich Pvt. Ltd. Isobutyltrimethylphosphonium bromide ($P_{111i4}Br$) ≥ 99% was purchased from Boron Molecular, Australia (Scheme 2).

Monomer synthesis: three different monomer molecules **4**, **5**, **6** were synthesized using a three step procedure described below.

Step 1: for the synthesis of 3-(chlorosulfonyl)propyl methacrylate (**2**), 15 g of potassium 3-(methacryloyloxy) propane-1-sulfonate/3-sulfopropyl methacrylate potassium salt (KSPM) was placed in a round bottomed flask filled with argon. 25 ml of anhydrous dry THF was added to the flask; to this solution, 1.7 ml of dry DMF (acts as a catalyst) was further added via a syringe. This whole reaction flask was maintained at 0 °C in an ice bath. Then, 39.9 g, 0.335 mol of thionyl chloride was added dropwise and the mixture was left stirring overnight. The obtained suspension was carefully added to ice water (approx. 200 mL, which was prepared by adding liquid N_2 to water in a clean flask); once the suspension settled down, the upper aqueous layer was decanted. The oily organic layer was diluted with 80 ml of dichloromethane (CH_2Cl_2), and the CH_2Cl_2 layer was then washed with brine water (6 × 25 mL) in a separating flask and dried with $MgSO_4$ with stirring for 1 hour. The $MgSO_4$ was filtered off under vacuum on a Schlenk line to obtain the product (**2**). Analysis: $C_7H_{11}ClO_4S$ (226.68): ^1H NMR (400.07 MHz, $CDCl_3$): δ = 6.09(s, 1H, CH_2=C(CH_3)–), 6.05 (s, 1H, CH_2=C(CH_3)–), 4.26(t, 2H, CO–O–CH_2–), 3.72(m, 2H, –$CH2$–SO_2Cl), 2.07(m, 2H, CO–O–CH_2–CH_2–), 1.89 (s, 3H, CH_2=C(CH_3)–)

Step 2: for the synthesis of triethyl ammonium 1-[3-(methacryloxy)propylsulfonyl]-1-(trifluoromethane-sulfonyl) imide **3**, trifluoromethanesulfonamide $NH_2SO_2CF_3$ (7.3 g, 0.049 mol) was placed in a round bottomed flask by flushing Ar, and anhydrous $N(C_2H_5)_3$ (10.9 g, 0.107 mol) was added under stirring. 40 ml of anhydrous THF was further added to the mixture and the resultant solution was cooled at 0 °C in an ice bath. 3-Chlorosulfonyl)propyl methacrylate (product **2**) (11.1 g, 0.049 mol) was dissolved in 15 mL of anhydrous THF. This solution was added dropwise to the solution of THF with $NH_2SO_2CF_3$ and $N(C_2H_5)_3$ under an inert atmosphere and the reaction was left stirring at 0 °C for 1 hour and at room temperature. The obtained precipitate was filtered off and the remaining THF was removed by using a rotavap and a slightly yellow oily residue was obtained, which was dissolved in

90 mL of CH_2Cl_2. The dichloromethane was washed with brine water (4 × 35 mL) and dried with $MgSO_4$. It was further filtered, and the excess dichloromethane was removed by a rotavap followed by drying under vacuum on a Schlenk line and stored in a refrigerator at 3.8 °C. Analysis: $C_{14}H_{27}F_3N_2O_6S_2$ (440.50): ^1H NMR (400.07 MHz, $CDCl_3$) δ = 6.02 (s, 1H, CH_2=C(CH_3)–), 5.69 (t, 1H, CH_2=C(CH_3)), 4.18 (t, 2H, CO–O–CH_2–), 3.16–2.99 (m, 8H, H–N (CH_2CH_3)$_3$ and CH_2–SO_2–N–), 2.05–1.97 (m, 2H, O–CH_2–CH_2–CH_2–), 1.89(s, 3H, CH_2=C(CH_3)–), 1.14 (t, 9H, H–N(CH_2CH_3)$_3$).

Step 3: for the synthesis of the Na monomer (NaMTFSI), **4**, 1.5 eq. of NaH (0.8 g, 0.033 mol) (purchased from Sigma Aldrich) was dissolved in 20 mL of anhydrous THF in an addition flask. In a round bottomed flask, 9.8 g of product **3** was dissolved in 30 mL of anhydrous THF in an ice bath (0 °C) under an inert atmosphere. The NaH solution was added dropwise to the product **3** solution. The reaction was left stirring for 2 hours at room temperature, and then unreacted NaH was removed by filtration, and THF was removed by a rotavap. The concentrated product **4** was washed with cyclohexane under vigorous stirring (3 × 20 mL) and the excess hexane was decanted. We obtained a yellow oily residual product **4**, to which dry dichloromethane was added until the oil residue dissolved. This sample was stored in a refrigerator overnight below 3.8 °C to form white crystals of a NaMTFSI monomer with a product yield of 48%. The white crystals were filtered off the next day, washed with diethyl ether and dried on a Schlenk line. Analysis: $C_8H_{11}F_3NO_6S_2$ (360.59) ^1H NMR (400.07 MHz, $CDCl_3$) δ = 6.02 (s, 1H, CH_2=C(CH_3)–), 5.69 (s, 1H, CH_2=C(CH_3)), 4.18(t, 2H, CO–O–CH_2–), 3.16 (t, CH_2–SO_2–N–), 2.05–1.97(m, 2H, O–CH_2–CH_2–CH_2–), 1.89(s, 3H, CH_2=C(CH_3)–).

P_{111i4}MTFSI monomer **5** was synthesised in a one-step procedure. Product **4** NaMTFSI (2.34 g, 0.0064 mol) was dissolved in 15 mL of Milli-Q water in a beaker. In a separate beaker, 1.5 eq. of $P_{111i4}Br$ (2.07 g, 0.0097 mol) was dissolved in 10 mL of Milli-Q water. The $P_{111i4}Br$ solution was added dropwise to a solution containing NaMTFSI using an addition flask and the reaction was kept stirring for 30–40 min at room temperature. While the reaction was going on, 15 mL of CH_2Cl_2 was added and the reaction was left stirring for an additional 1 hour at room temperature. The upper aqueous layer was decanted. The oily residue was washed with brine water (3 × 15 mL) to remove excess CH_2Cl_2 and then it was further dried with $MgSO_4$ and filtered. The obtained viscous oily layer was further subjected to rotavap drying to remove any residue of CH_2Cl_2; 0.01 M hydroquinone inhibitor was added before rotavap drying to avoid self-polymerisation. Product **5** finally underwent an additional drying step under vacuum on a Schlenk line and finally stored in the refrigerator at <5 °C. Analysis: $C_{16}H_{32}F_3NO_6S_2$ (471.25) ^1H NMR (400.13 MHz, $CDCl_3$) 6.02 (s, 1H, CH_2=C(CH_3)–), 5.49 (s, 1H, CH_2=C(CH_3)), 4.18 (t, 2H, CO–O–CH_2–), 3.16 (m, CH_2–SO_2–N–), 2.19–2.05 ((m, 2H, O–CH_2–CH_2–CH_2–)+(2H–CH–CH_2)), 2.01–1.939 (m, CH_3–CH–CH_3), 1.891 (s, 3H, CH_2=C(CH_3)–), 1.87–1.84 (s, 3H, CH_3–P–, CH_3–P–, CH_3–P–), 1.05 (s, 3H CH_3–CH–), 1.02 (s, 3H CH_3–CH–).

© 2024 The Author(s). Published by the Royal Society of Chemistry

RSC Appl. Polym., 2024, **2**, 384–394 | **391**

P_{122i4}MTFSI monomer **6** was synthesised in a one-step procedure. Product **4** NaMTFSI (2.0 g, 0.0055 mol) was dissolved in 15 mL of Milli-Q water in a beaker, while in a separate beaker, 1.5 eq. of P_{122i4}TSO (2.75 g, 0.0083 mol) was dissolved in 10 mL of Milli-Q water. The P_{122i4}TSO solution was added dropwise to a solution containing NaMTFSI through an addition flask and the reaction was kept stirring for 30–40 min at room temperature. While the reaction was still going on, 15 mL of CH_2Cl_2 was added and the reaction mixture was left stirring for an additional 1 hour at room temperature. The upper aqueous layer was subsequently decanted and the oily residue was washed with brine water (3 × 15 mL) to remove excess CH_2Cl_2, and then it was further dried with $MgSO_4$ and filtered off. The obtained viscous oily layer was further subjected to rotavap drying to remove any residue of CH_2Cl_2, and then 0.01 M hydroquinone inhibitor was added before rotavap drying to avoid self-polymerisation. Product **6** was finally extra dried under vacuum on a Schlenk line and stored in the refrigerator. Analysis: $C_{17}H_{33}F_3NO_6PS_2$ (499.54) ^{1}H NMR (400.13 MHz, $CDCl_3$) δ = 6.02 (s, 1H, CH_2=C(CH_3)–), 5.69 (s, 1H, CH_2=C(CH_3)), 4.18 (t, 2H, CO–O–CH_2–), 3.16 (m, CH_2–SO_2–N–), 2.29–2.15 (m, 4H, CH_3–CH_2–P–CH_2–CH_3), 2.08 (s, 2H CH_2–C–CH_3), 2.00 (m, 2H, O–CH_2–CH_2–CH_2–), 1.87 (s, 3H, CH_3–P–CH_2), 1.26–1.10 (m, CH_3–CH_2–P–CH_2–CH_3), 1.05 (s, CH_2=C(CH_3)), 1.04–1.02(s, 6H CH_3–C–CH_3), 0.8(s, 2H, P–CH_2–C–CH_3).

Polymer synthesis routes

The polymerisation of NaMTFSI **7** was done in water as a solvent in a 1 : 1 ratio as follows: 2.0 g of NaMTFSI was dissolved in 2 mL of Milli-Q water and to this solution, 0.02 g of 4,4′-azobis(4-cyanovaleric acid) initiator was added. The solution was mixed well and degassed with Ar gas for 1 hour, and the reaction flask was covered with Al foil to avoid light as the initiator is light sensitive. After degassing, the reaction flask was immersed in an oil bath at 80 °C and left overnight. After the polymerisation was completed, the water was removed with a rotavap and excess water was removed using a lyophilizer before drying on the Schlenk line. Finally the white product **7** with 35% yield was obtained and stored in an argon-filled glove box. Analysis: $C_8H_{11}F_3NO_6S_2$ (360.59) ^{1}H NMR (400.07 MHz, DMSO) δ = 3.06 (m, 2H, O–CH_2–CH_2–CH_2–), 1.956 (t, CH_2–SO_2–N–), 1.17 (t, 2H, CO–O–CH_2–), 1.08 (s, 1H, CH–C(CH), 1 g of product **6** was dissolved in 1 mL of DMF; to this solution, 0.01 g of AIBN was added as the initiator, and then the solution was mixed well and degassed with Ar gas for 1 hour before the reaction flask was immersed in an oil bath at 90 °C and left overnight. After polymerisation the obtained polymer was washed with diethyl ether (2 × 40 mL); the final product **8** was further dried under vacuum on a Schlenk line and stored in an argon-filled glove box. Analysis: $C_{16}H_{32}F_3NO_6S_2$ (471.25) ^{1}H NMR (400.07 MHz, DMSO) δ = 3.06 (m, 2H, O–CH_2–CH_2–CH_2–), 2.05 (t, 2H–CH–CH_2)), 2.01–1.939 (m, CH_3–CH–CH_3), 1.956(t, CH_2–SO_2–N–), 1.891 (s, 3H, CH_2=C(CH_3)–), 1.87–1.84(s, 3H, CH_3–P–, CH_3–P–, CH_3–P–),

1.17(t, 2H, CO–O–CH_2–), 1.08 (s, 1H, CH–C(CH)), 1.05 (s, 3H CH_3–CH–), 1.02 (s, 3H CH_3–CH–).

Polymer **7** was similarly prepared from monomer **5** with a 35% yield and dried as above, before being stored in an argon filled glove box. Analysis: $C_{17}H_{33}F_3NO_6PS_2$ (499.54) ^{1}H NMR (400.13 MHz, DMSO) δ = 3.06 (m, 2H, O–CH_2–CH_2–CH_2–), 2.29–2.15 (m, 4H, CH_3–CH_2–P–CH_2–CH_3), 2.08 (s, 2H CH_2–C–CH_3), 2.00 (m, 2H, O–CH_2–CH_2–CH_2–), 1.956 (t, CH_2–SO_2–N–), 1.87 (s, 3H, CH_3–P–CH_2), 1.26 (m, CH_3–CH_2–P–CH_2–CH_3), 1.17 (t, 2H, CO–O–CH_2–), 1.08 (s, 1H, CH–C(CH)), 1.04–1.02 (s, 6H CH_3–C–CH_3), 0.8 (s, 2H, P–CH_2–C–CH_3). The formation of polymers **7**, **8** and **9** was analysed with the help of ^{1}H NMR as shown in Fig. S3.† All the three polyelectrolytes were amorphous in nature.

Electrolyte membrane preparation

The electrolyte membrane was prepared by mixing poly NaMTFSI (**7**) with poly-P_{111i4}MTSFI (**8**) and poly-P_{122i4}MTSFI (**9**) in acetonitrile separately. The different ratios used are summarised in Table 1. Once the homogeneous mixture was formed, the solvent was removed completely under vacuum under an Ar atmosphere and dried. The dried powder was then hot pressed at different temperatures ranging from 70 to 100 °C to obtain the electrolyte membrane. Once the membrane was formed, it was further dried under vacuum to remove any residual solvents and stored in an Ar filled glove box.

Instrumentation

Differential scanning calorimetry (DSC). A Netzsch DSC (214 Polyma) was used to measure the thermal properties of the polymer blends. All samples were weighed (approx. 10–15 mg) and sealed in Al pans in an Ar-filled glove box. Cyclohexane was used to calibrate the instrument. All the samples were measured at a heating rate of 10 K min^{-1} in the temperature range −40 to 160 °C. The mid-point from the second heating trace was used for the study of T_g in all the materials.

Ionic conductivity. The ionic conductivity was measured by Ac impedance spectroscopy using MTZ-35 within a frequency range of 1 Hz to 10 MHz and a voltage of 0.01 V within the temperature range of 50–90 °C. The electrolyte membrane was cut to 12 mm diameter, sandwiched between two stainless steel blocking electrodes and then placed inside a custom-built barrel cell. All the spectra were fitted using MT-lab software.

Dynamic mechanical analysis (DMA). A DMA 8000 (PerkinElmer) was used to study the mechanical properties of the electrolyte membrane. In this study we focused on one composition 50 : 50 mol% polymer blends of poly-NaMTFS: poly-P_{111i4}MTFSI and poly-NaMTFSI: poly-P_{122i4}MTFSI. The sample was studied in the temperature range of 30 to 150 °C. The sample was first cooled and then heated at 2 K min^{-1}. The sample was cut into 1.5 × 5 mm. The storage modulus and tan (δ) were determined using tensile mode with a frequency of 1 Hz and an elongation of 0.02 mm.

392 | *RSC Appl. Polym.*, 2024, **2**, 384–394

© 2024 The Author(s). Published by the Royal Society of Chemistry

Electrochemical characterisation of 30 mol% NaFSI salt as a plasticizer in a 50 : 50 mol% polymer blend of poly-P$_{111i4}$MTFSI and poly-NaMTFSI

Na$^+$ transference number measurement (T_{Na^+}). T_{Na^+} was measured by using the Bruce–Vincent method.[27] The equivalent circuit for interfacial resistance was fitted by using the circuit as shown below:

where R_1 is the bulk resistance of the electrolyte. R_2 and R_3 represent the resistance related with two electrode surfaces. The EC-Lab V11.27 software was used to analyse the data and the fitting method is Randomize + Simplex.

Author contributions

Sneha Malunavar: experiments, data analysis, and writing – original draft. Luca Porcarelli: methodology design and supervision. Patrick Howlett: project conceptualization, manuscript editing and supervision, David Mecerreyes: conceptualization of polymer synthesis and contribution to manuscript editing, and Maria Forsyth: project conceptualization, analysis and interpretation of data, and manuscript preparation.

Conflicts of interest

There are no conflicts of interest.

Acknowledgements

References

1 M. Armand and J.-M. Tarascon, *Nature*, 2008, **451**, 652–657.
2 J. W. Choi and D. Aurbach, *Nat. Rev. Mater.*, 2016, **1**, 16013.
3 X. Chen, Z. Guan, F. Chu, Z. Xue, F. Wu and Y. Yu, *InfoMat*, 2022, **4**(1), e12248.
4 C. Zhao, J. Guo, Z. Gu, X. Wang, X. Zhao, W. Li, H. Yu and X. Wu, *Nano Res.*, 2022, **15**(2), 925–932.
5 M. Yu, Z. Gu, J. Guo, C. Wang and X. Wu, *Chem. Commun.*, 2022, **58**, 6813–6816.
6 D. E. Fenton, J. M. Parker and P. V. Wright, *Polymer*, 1973, **14**, 589.
7 W. Gorecki, M. Jeannin, E. Belorizky, C. Roux and M. Armand, *J. Phys.: Condens.Matter*, 1995, **7**, 6823–6832.
8 V. Di Noto, S. Lavina, G. A. Giffin, E. Negro and B. Scrosati, *Electrochim. Acta*, 2011, **57**, 4–13.
9 C. Li, H. Zhang, L. Otaegui, G. Singh, M. Armand and L. M. Rodriguez-Martinez, *J. Power Sources*, 2016, **326**, 1–5.
10 E. Quartarone and P. Mustarelli, *Chem. Soc. Rev.*, 2011, **40**, 2525–2540.
11 A. M. Stephan, *Eur. Polym. J.*, 2006, **42**, 21–42.
12 J. W. Fergus, *J. Power Sources*, 2010, **195**, 4554–4569.
13 J. Yuan, D. Mecerreyes and M. Antonietti, *Prog. Polym. Sci.*, 2013, **38**, 1009–1036.
14 A. S. Shaplov, R. Marcilla and D. Mecerreyes, *Electrochim. Acta*, 2015, **175**, 18–34.
15 D. Mecerreyes, *Prog. Polym. Sci.*, 2011, **36**, 1629–1648.
16 X. G. Sun, J. B. Kerr, C. L. Reeder, G. Liu and Y. Han, *Macromolecules*, 2004, **37**, 5133–5135.
17 M. Doyle, T. F. Fuller and J. Newman, *Electrochim. Acta*, 1994, **39**, 2073–2081.
18 D. J. Bannister, G. R. Davies, I. M. Ward and J. E. McIntyre, *Polymer*, 1984, **25**, 1291–1296.
19 H. Zhang, C. Li, M. Piszcz, E. Coya, T. Rojo, L. M. Rodriguez-Martinez, M. Armand and Z. Zhou, *Chem. Soc. Rev.*, 2017, **46**, 797–815.
20 S. Zheng, Q. Liu and L. Yang, *Polymer*, 1994, **35**, 3740–3744.
21 S. A. Mohd Noor, D. Gunzelmann, J. Sun, D. R. MacFarlane and M. Forsyth, *J. Mater. Chem. A*, 2014, **2**, 365–374.
22 S. A. M. Noor, J. Sun, D. R. Macfarlane, M. Armand, D. Gunzelmann and M. Forsyth, *J. Mater. Chem. A*, 2014, **2**, 17934–17943.
23 C. R. Pope, K. Romanenko, D. R. MacFarlane, M. Forsyth and L. A. O'Dell, *Electrochim. Acta*, 2015, **175**, 62–67.
24 Y. V. Oza, D. R. Macfarlane, M. Forsyth and L. A. O'Dell, *Electrochim. Acta*, 2015, **175**, 80–86.
25 A. S. Shaplov, P. S. Vlasov, M. Armand, E. I. Lozinskaya, D. O. Ponkratov, I. A. Malyshkina, F. Vidal, O. V. Okatova, G. M. Pavlov, C. Wandrey, I. A. Godovikov and Y. S. Vygodskii, *Polym. Chem.*, 2011, **2**, 2609–2618.
26 L. Porcarelli, A. S. Shaplov, M. Salsamendi, J. R. Nair, Y. S. Vygodskii, D. Mecerreyes and C. Gerbaldi, *ACS Appl. Mater. Interfaces*, 2016, **8**, 10350–10359.
27 J. Evans, C. A. Vincent and P. G. Bruce, *Polymer*, 1987, **28**, 2324–2328.
28 G. J. Tudryn, W. Liu, S. W. Wang and R. H. Colby, *Macromolecules*, 2011, **44**, 3572–3582.
29 W. Wang, G. J. Tudryn, R. H. Colby and K. I. Winey, *J. Am. Chem. Soc.*, 2011, **133**, 10826–10831.

© 2024 The Author(s). Published by the Royal Society of Chemistry

RSC Appl. Polym., 2024, **2**, 384–394 | 393

30 Y. Wang, A. L. Agapov, F. Fan, K. Hong, X. Yu, J. Mays and A. P. Sokolov, *Phys. Rev. Lett.*, 2012, **108**, 1–5.

31 G. Huang, L. Porcarelli, Y. Liang, M. Forsyth and H. Zhu, *ACS Appl. Energy Mater.*, 2021, **4**, 10593–10602.

32 O. Danyliv and A. Martinelli, *J. Phys. Chem. C*, 2019, **123**, 14813–14824.

33 S. A. Mohd Noor, D. Gunzelmann, J. Sun, D. R. MacFarlane and M. Forsyth, *J. Mater. Chem. A*, 2014, **2**, 365–374.

34 S. Malunavar, A. Gallastegui, X. Wang, F. Makhlooghiazad, D. Mecerreyes, M. Armand, M. Galceran, P. C. Howlett and M. Forsyth, *ACS Appl. Polym. Mater.*, 2022, **4**(12), 8977–8986.

35 P. G. Bruce, M. T. Hardgrave and C. A. Vincent, *Solid State Ionics*, 1992, **53–56**, 1087–1094.

36 Z. Xue, D. He and X. Xie, *J. Mater. Chem. A*, 2015, **3**, 19218–19253.